

# Synthesis of nanocrystalline cubic $\text{ZrO}_2\text{:Mn}^{2+}$ phosphors: Structural and luminescent properties

A. Fernández-Osorio\*, L. Ramos-Olmos\*, Julián C.F.\*

Universidad Nacional Autónoma de México C.P. 54740 Edo de Méx., México, \*ana8485@unam.mx  
, \*\* lulu80@unam.mx, \*\*\*juchafe76@unam.mx

## ABSTRACT

Nanocrystalline cubic zirconia doped with manganese, solid solutions of  $\text{Zr}_{1-x}\text{Mn}_x\text{O}_{2-x/2}$  ( $x=0, 0.1, 0.2$  and  $0.4$ ), were prepared by the sol-gel method. The Rietveld refinement of the X-ray powder diffraction (XRD) profile of the samples confirms the stabilization of zirconia in the cubic phase, and the data show the presence of the solid solution as well as oxygen vacancies in the lattice. The crystallite average size of this system is  $5.0 \pm 2.0$  nm, as determined by XRD, which is in close agreement with the particle size determined by high-resolution transmission electronic microscopy (HRTEM). The luminescence properties of these nanophosphors were characterized by their excitation and emission spectra. The photoluminescent spectra exhibited a prominent blue emission band centered at 465 nm, corresponding to the  $4\text{T}_1-6\text{A}_1$  transition of  $\text{Mn}^{2+}$  under an excitation wavelength of 260 nm.

**Keywords:** manganese-stabilized cubic zirconia, phosphors,  $\text{ZrO}_2$  nanoparticles

## 1 INTRODUCTION

Oxide phosphors have been widely used in modern lighting and display parts, such as fluorescent lamps, cathode-ray tubes, field emission displays and plasma display panels.

Fluorescent nanoparticles continue to garner great interest as materials for use in optoelectronic devices and fluorescent biomarkers.

Zirconium dioxide ( $\text{ZrO}_2$ ) is very interesting from a technological point of view, since it can be used as a structural ceramic, a solid electrolyte, a gas sensor, and as a catalyst. Decreasing the size of zirconia-based particles to nanometric levels provides significant changes in their physical and chemical properties due to modifications produced at structural or electronic levels.

Interest in nanocrystalline zirconia with an average grain size below 10 nm has increased during the past few years because their properties often differ significantly from those of the bulk zirconia.

Pure bulk  $\text{ZrO}_2$  exhibits three structures in different ranges of temperature at atmospheric pressure. The most stable thermodynamic form is monoclinic and transforms to

tetragonal and cubic (fluorite) structures at 1400 and 2700 K (up to the melting point of 2950 K), respectively.

However, pure  $\text{ZrO}_2$  is unstable in the cubic or tetragonal phase at room temperature. Addition a suitable cation into the  $\text{ZrO}_2$  is known to stabilize these meta stable phases by creating oxygen vacancies to yield energetically favored structures.

Extensive effort has focused on the preparation of stabilized cubic and tetragonal zirconia by the addition of various ions (e.g.,  $\text{Y}^{3+}$ ,  $\text{Ce}^{4+}$ ,  $\text{Ti}^{4+}$  and  $\text{Ca}^{2+}$ ), trivalent and divalent cations to form oxygen vacancies that preserve electrical neutrality [1]

Another mechanism for stabilizing c- $\text{ZrO}_2$  exploits the size effect to generate nanocrystalline c- $\text{ZrO}_2$  with an average grain size of 15 nm predominantly in powder form.

Interest in nanocrystalline zirconia, with an average grain size below 10 nm, has increased during the past few years, because their properties are often significantly different from those of bulk zirconia [2].

It is known that the luminescence of rare-earth and transition metal ions depend on the  $\text{ZrO}_2$  crystalline structure, and the  $\text{ZrO}_2$  tetragonal and cubic structures can be stabilized by the incorporation of these ions.

The synthesis of nanocrystalline  $\text{ZrO}_2$  phosphors, mostly in powder form, has been achieved via a range of different methods, including chemical vapor deposition, sol-gel techniques, microwave irradiation, spray pyrolysis and hydrothermal synthesis, among others [3]. Although the synthesis of zirconia nanoparticles is widely established in literature, the as-synthesized materials obtained by these methods are typically amorphous or mixed-phase zirconia nanoparticles.

The present work reports a novel and easy pathway for the synthesis of nanostructured manganese-stabilized cubic zirconia ( $\text{MnSZ}$ ) powders, the solid solution containing  $\text{Zr}_{1-x}\text{Mn}_x\text{O}_{2-x/2}$  ( $x=0, 0.03, 0.06$ , and  $0.09$ ) nanoparticles with an average size of  $6 \pm 2.0$  nm, prepared by the sol-gel method, we provide results from a structural study and a description of their luminescent properties.

## 2 EXPERIMENTAL

### 2.1 Sample preparation

The  $Zr_{1-x}Mn_xO_{2-x/2}$  solid solutions ( $x=0, 0.03, 0.06,$  and  $0.1$ ) were prepared by the sol-gel method. The starting materials zirconium (IV) propoxide  $Zr(OCH_2CH_2CH_3)_4$  and manganese (II) acetate tetrahydrate  $(CH_3CO_2)_2Mn \cdot 4H_2O$  were both provided by Aldrich (99.99%) and used in a stoichiometric molar ratio. The procedure used to prepare the nanosized  $ZrO_2:Mn^{2+}$  is as follows.

#### a) Un-doped $ZrO_2(x=0)$

De-ionized water was added dropwise to 8ml of zirconium propoxide until the pH value reached 9.0, producing a white polymeric gel. The gel was dried at room temperature for five days; when completely dry, it was ground in an agate mortar and annealed in argon for 2 h at 300°C, 400°C, and 500°C. After each annealing, the sample was analyzed using X-ray powder diffraction.

#### b) $Zr_{0.97}Mn_{0.03}O_{1.98}$ , $Zr_{0.94}Mn_{0.06}O_{1.97}$ , and $Zr_{0.91}Mn_{0.09}O_{1.95}$

Stoichiometric amounts of manganese (II) acetate tetrahydrate  $(CH_3CO_2)_2Mn \cdot 4H_2O$  were dissolved in 2-methoxyethanol  $CH_3O(CH_2)_2OH$  (99.9%, Aldrich). After 30 min of stirring, zirconium propoxide was added to this solution, followed by de-ionized water. At a pH value of 9.0, a white gel was obtained. This gel was dried at room temperature for five days; when completely dry, it was ground in an agate mortar and annealed in argon for 2 h at 300°C, 400°C and 500°C. After each annealing, the samples were analyzed with X-ray powder diffraction.

### 2.2. Characterization

X-ray diffraction data were obtained with a Siemens D5000 diffractometer with Cu  $K\alpha$  radiation. Intensities were obtained in the  $2\theta$  ranges between 2.5° and 70° with a step of 0.02° and a measuring time of 0.4 s per point. The average crystallite sizes of the MnSZ nanopowders was estimated using the Scherrer equation, taking into account the broadening of the X-ray diffraction peaks over all reflections.

The Rietveld refinement of the powder profiles was performed using TOPAS academic software [26]. The XRD data of the  $Zr_{1-x}Mn_xO_{2-y}$   $x=0.06$  samples annealed in argon at 500 and 700°C underwent peak fitting using TOPAS (Bruker AXS 2004) were obtained in the  $2\theta$  range of 10–110° using a step-scan mode with a step size of 0.05° and a counting time of 30 s per step.

The excitation and emission spectra were obtained on an F-7000 spectrometer (Hitachi) equipped with a 150-W xenon lamp as the excitation source. High-resolution transmission electron microscopy (HR-TEM). The micrographs were obtained in a JEOL-2000F analytical microscope, operating at 200 kV by depositing sample powder dispersed in methanol onto a 200-mesh Cu grid coated with a carbon layer.

## 3 RESULTS AND DISCUSSION

### 3.1 Phase composition and crystal structure

When the samples were annealed below 400°C, amorphous material was produced that crystallized after heating at 500°C. In the un-doped sample, the crystallized phases were a mixture of monoclinic and cubic zirconia polymorphs.

When the doped samples were annealed at 500°C, the amorphous structure crystallized to form nanocrystalline cubic zirconia. The XRD patterns of the as-synthesized MnSZ at 3, 6 and 9 mol% manganese match those of pure cubic zirconia, indicating the formation of a single phase (Fig.1).

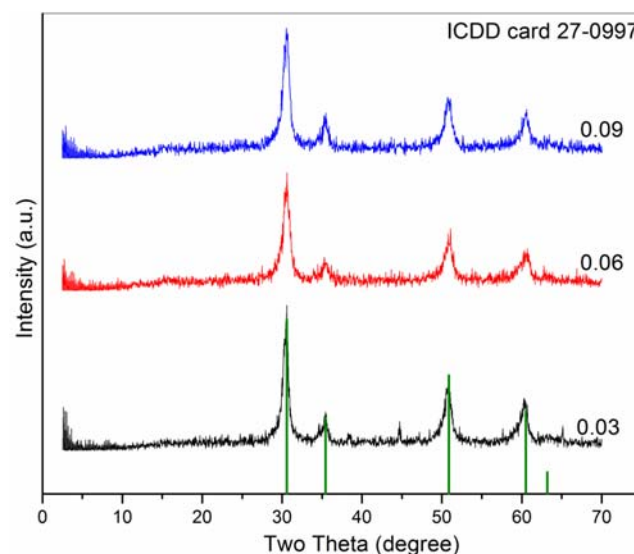


Fig.1 X-ray diffraction patterns for the different manganese concentrations calcinated at 500°C

The average particle size of these samples is of  $6 \pm 2.0$  nm. The X-ray powder diffraction pattern of the  $Zr_{1-x}Mn_xO_{2-x/2}$   $x=0.06$  sample heated in argon for 2 h at 500°C was scanned in the  $2\theta$  range of 10–110° using a step-scan mode with a step size of 0.05° and a counting time of 30 s per step, is shown in Figure 2.

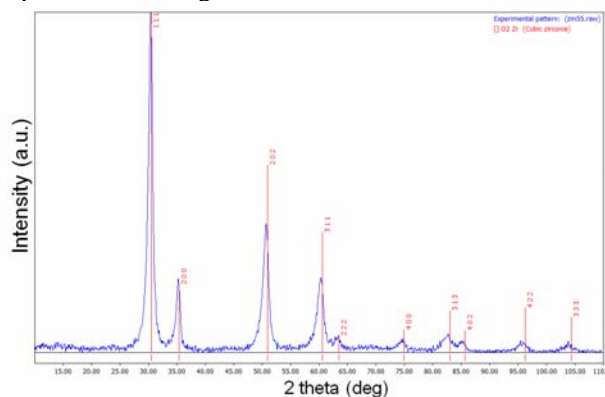


Fig.2. X-ray powder diffraction of MnSZ (6 mol % Mn) sample annealed at 500°C

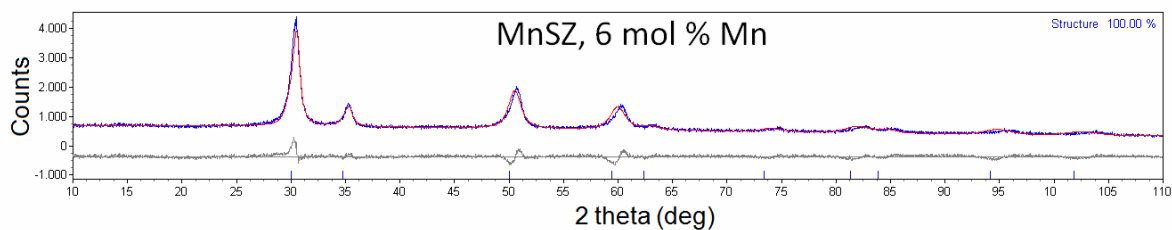


Fig.3. X-ray pattern and Rietveld curve for the MnSZ (6 mol % Mn) sample

All diffraction peaks could be perfectly indexed to cubic zirconium oxide (ICDD 27-0997) with a unit symmetry described by the space group Fm3m and a lattice parameter  $a = 5.09 \text{ \AA}$ . The desired cubic phase is the only phase present under these heat treatment conditions

The average crystallite size using the Scherrer equation, taking into account the broadening of the X-ray diffraction peaks over all reflections in this sample is of 6.2 nm

Researchers have explained formation of this metastable phase at low temperature by various theories involving stabilization because of the defects/atomic vacancies in the lattice created by the presence of lower valent doped metal ions.

The Rietveld refinement technique was used to determine the phase composition and verify the site occupation of  $\text{Mn}^{2+}$  in the cubic structure of the samples  $\text{Zr}_{1-x}\text{Mn}_x\text{O}_{2-x/2}$   $x = 0.03, 0.06$  and  $0.09$  heated at  $500^\circ\text{C}$ , 2h.

The structural refinement of samples was performed with the powder data using Topas (Bruker AXS 2004) a complete powder pattern fitting software package. The instrumental and sample profiles were performed by a convolution of Lorentzian and Gaussian components, and the TCH pseudo Voigt profile function was used.

The XRD patterns of the samples confirm a single-phase cubic structure, and XRD refinements were continuous until convergence was reached with a goodness factor close to 1. Rietveld refinement of the samples was carried out using one model based on the Fm3m space group with ( $\text{Zr}^{4+}, \text{Mn}^{2+}$ ) and  $\text{O}^{2-}$  ions in the special positions 4(a) and 8(c), respectively. Several constraints were applied at the start of the refinement. The thermal parameters were constrained to be the same for all atoms sharing a particular site, and the total occupancy of sites was set to unity. The X-ray pattern and Rietveld curve for the  $\text{Zr}_{1-x}\text{Mn}_x\text{O}_{2-y}$   $x = 0.06$  sample annealed in argon at  $500^\circ\text{C}$  are provided in Fig.3.

The parameters obtained in the refinement, are summarized in Table 1.

Table 1

Structural parameters of MnSZ 3, 6 and 9 mol % Mn samples determined by Rietveld refinement

Parameters	x= 0.03	x= 0.06	x= 0.09	
Space group	Fm3m	Fm3m	Fm3m	
Lattice parameter, a (Å)	5.093	5.091	5.089	
Occupation parameters				
Atom	Wyckoff			
Zr	4a	0.9848	0.9787	0.9554
Mn	4a	0.016	0.0291	0.041
O	8c	0.9952	0.9963	0.9974
r.m.s. strain $\times 10^3$	2.921	3.015	3.018	
Agreement factors				
$R_{wp}$	7.91	8.17	8.32	
$R_p$	6.21	6.25	6.35	
$R_B$	1.79	1.81	1.89	

The obtained  $R_{Bragg}$  indices confirm the high quality of the structure model. The results of the refinement of the powder XRD profiles of the MnSZ samples suggest stabilization of MnSZ in the cubic phase with 3, 6 and 9 mol % manganese. The values obtained of the occupancy factor for zirconium and manganese atoms in the c-MnSZ with 3, 6 and 9 mol % Mn annealed at  $500^\circ\text{C}$ , confirm the presence of  $\text{Mn}^{2+}$  ions in the zirconia lattice. The lattice parameters of the samples are similar to  $5.090 \text{ \AA}$  value for un-doped  $\text{ZrO}_2$ . No decrease in lattice parameter was observed, according to their ionic radii,  $\text{Mn}^{2+}$  ions ( $0.80 \text{ \AA}$ ) should replace  $\text{Zr}^{4+}$  ( $0.79 \text{ \AA}$ ) in the normal sites of the lattice. In a fluorite-type solid solution, replacing the host cation with a foreign cation with a different radius and valence state introduces strain. Substituting the  $\text{Zr}^{4+}$  with a smaller ion leads to a contraction of the lattice, and the incorporation of a larger ion leads to an increase in the lattice parameter. The values obtained of the occupancy factor for zirconium and manganese atoms in the c-MnSZ, confirm the presence of  $\text{Mn}^{2+}$  ions in the zirconia lattice.

### 3.2 High-resolution transmission electron micrographs (HR-TEM)

The HR-TEM micrographs corroborate the formation of small nanocrystals with dimensions close to those determined by X-ray diffraction patterns. Representative nanocrystallites obtained from c-MnSZ (6 mol % Mn) powders annealed in argon at 500°C are shown in Figure 4.

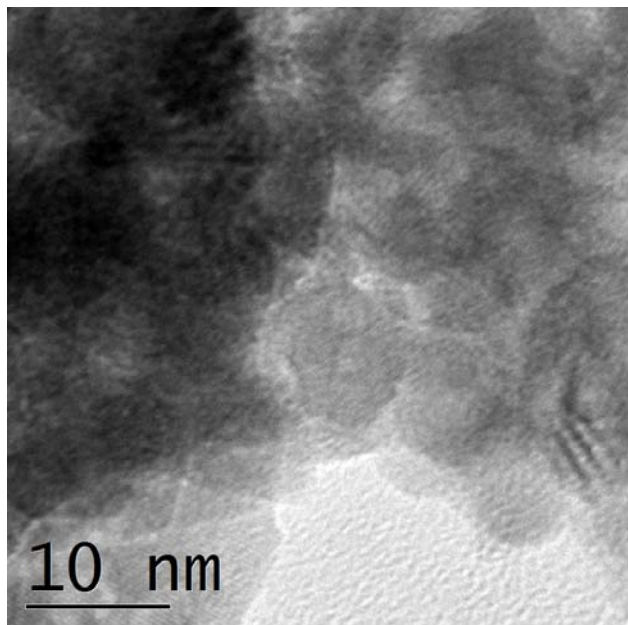


Fig.4. HR-TEM image of the MnSZ (6 mol % Mn) powders annealed at 500°C

Most of the zirconia nanoparticles have spherical morphologies without highly aggregated particles. The observed diameter of the spherical nanocrystals is approximately 6 nm, which is consistent with that calculated using the XRD data.

### 3.3 Photoluminescence spectra

The emission spectra of  $\text{ZrO}_2:\text{Mn}^{2+}$  ( $x=0.03, 0.06, \text{ and } 0.09$ ) nanophosphors heated in argon for 2 h at 500°C, under the excitation wavelength of 260 nm were shown in Figure 5.

Both phosphors exhibit blue emission between 400 and 650 nm, the samples exhibit a broad emission band with a maximum approximately 460 nm corresponding to the  ${}^4\text{T}_1$  ( ${}^4\text{G}$ )  $\rightarrow$   ${}^6\text{A}_1$  ( ${}^6\text{S}$ ) transition of the  $\text{Mn}^{2+}$  ion in the fluorite structure. It is well known that this transition is both spin and parity forbidden. From this figure, it can be found that the emission intensity increase with increasing the manganese concentration in  $\text{ZrO}_2$  host. We were unable to

obtain the spectrum of un-doped cubic  $\text{ZrO}_2$  because this synthesis route led to a mixture of zirconia polymorphs.

These results confirm the substitution of  $\text{Mn}^{2+}$  ions for  $\text{Zr}^{4+}$  in the zirconia host lattice and the formation of  $\text{Zr}_{1-x}\text{Mn}_x\text{O}_{2-x/2}$  solid solutions.

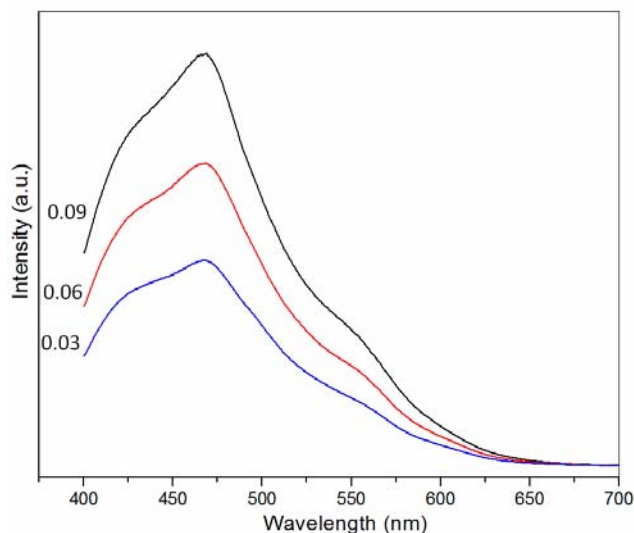


Fig.5. PL spectra of the MnSZ samples at 3, 6 and 9 mol % manganese concentration

## 4 CONCLUSIONS

Using the synthesis method described in the present work, for the system  $\text{Zr}_{1-x}\text{Mn}_x\text{O}_{2-x/2}$   $x=0.03, 0.06$  and  $0.09$ , nanocrystalline single-phase of cubic stabilized zirconia, with an average crystallite size of  $6\pm 2.0$  nm, was produced. The Rietveld refinement confirmed the formation of solid solutions with fluorite structure.

Concentrations of 3, 6 and 9 mol% manganese stabilize the cubic zirconia, and the small crystallite size is also an important factor in the stabilization of the zirconia in the cubic phase.

The PL spectra show blue emission bands, the intensity increase with increasing manganese concentration, the optimal concentration of  $\text{Mn}^{2+}$  is 9 mol %.

### Acknowledgments

The authors wish to thank the CONACYT CB-2011/165539 project for financial support.

## REFERENCES

- [1] Winterer, M. Nanocrystalline Ceramics: Synthesis and Structure; Springer: Berlin, Germany, 129-183, 2002.
- [2] M. Lajavardi, D.J. Kenney, S.H. Lin, J. Chin. Chem. Soc. 47 1055-1063, (2000).
- [3] H. Zhang, X. Fu, S. Niu, et al., Mater. Chem. Phys. 91, 361-364 (2005).